We are IntechOpen, the world's leading publisher of Open Access books Built by scientists, for scientists

4,800
Open access books available

122,000
International authors and editors

135M
Downloads

Our authors are among the

154
Countries delivered to

TOP 1%
most cited scientists

12.2%
Contributors from top 500 universities

CLARIVATE ANALYTICS BOOK CITATION INDEX INDEXED

WEB OF SCIENCE™

Selection of our books indexed in the Book Citation Index in Web of Science™ Core Collection (BKCI)

Interested in publishing with us?
Contact book.department@intechopen.com

Numbers displayed above are based on latest data collected.
For more information visit www.intechopen.com

Chapter 4

Evaluation of the Biotribological Behavior and Cytotoxicity of Laser-Textured ISO 5832-1 Stainless Steel for Use in Orthopedic Implants

Eurico Felix Pieretti, Andrea Cecília Dorión Rodas, Renato Altobelli Antunes and Maurício David Martins das Neves

Additional information is available at the end of the chapter

http://dx.doi.org/10.5772/intechopen.73140

Abstract

This chapter evaluated the influence of laser texturing process on the tribological behavior of the ISO 5832-1 austenitic stainless steel (SS). The friction coefficient and wear were determined using ball-cratering wear tests. The laser texturing process was carried out with a nanosecond optical fiber ytterbium laser at four different pulse frequencies. Cytotoxicity tests were carried out to determine if laser texturing affects the biomaterial biocompatibility. For comparison reasons, pristine surfaces were also evaluated. The results indicated that the wear volume and friction coefficient were reduced after laser texturing. The samples were considered noncytotoxic according to the biocompatibility tests as the laser texturing process did not decrease cell's viability.

Keywords: biomaterials, cytotoxicity, laser texturing, stainless steel, tribology

1. Introduction

Implantable medical devices used in mobile joints of the human body as well as for dental purposes require biocompatibility with the surrounding tissues and organs, mechanical strength, and corrosion resistance. The body fluids constitute a hostile environment for the implant, which is also subjected to various loads. The implant can release particles due to corrosion, corrosion associated with fatigue, and even friction against implantable components, bones, or other body parts. By coming into contact with the body fluids, these particles can be placed in locations far from the removed source causing complications to the patients.

Okasaki [1] evaluated the properties of metallic biomaterials with regard to the effect of friction on anodic polarization. He observed that corrosion was accelerated in the frictional environment with respect to static conditions. This effect was due to the formation of anodic areas in the stressed regions under friction whereas its periphery is cathodic.

Metallic particles released from the corrosion process may move passively, through tissue and/or circulatory system or can be transported in an active way when metabolized by macrophages [2]. In either case, this mass transport may lead to debris accumulation in surrounding tissues or even remote sites where they can participate in undesirable biological reactions, compromising biomaterial's biocompatibility.

Interaction between metallic implants and the human body can be affected by numerous factors such as the structure of the metal surface, its mechanical properties, size, and shape. When in contact with the body tissues after implantation, metallic devices affect the intensity of stresses to which the whole human body is subjected as well the implant itself. Wear and corrosion processes are additional effects arising from the interaction between metallic biomaterials and the body tissues [3].

The orthopaedic implants are projected and manufactured so that when used under the conditions and for the purposes designed, without compromising the clinical condition or the safety of patients. Any risks that may be associated with the implants use are acceptable when compared to benefits for the patients [2, 3].

The alloy described in part 1 of ISO 5832 [4] (ASTM F138/ASTM F139) is an austenitic stainless steel. It is one of the metallic materials most used in Brazil for manufacturing implants, because of its suitable mechanical strength, reasonable corrosion resistance, and low cost [5–8]. Stainless steel implantable medical devices are used as permanent or temporary implants to help bone healing. The laser texturing process is used to modify the biomaterial surface roughness and hardness.

The microscale abrasion test (or ball-cratering wear test) is a practical method to analyze the wear resistance of materials [8–11]. The ball-cratering wear test has gained large acceptance at universities and research centers and is widely used in studies focusing on the abrasive wear behavior of different materials [12–16]. **Figure 1** presents a schematic diagram of the principle of this wear test, where a rotating ball is forced against the specimen being tested and an

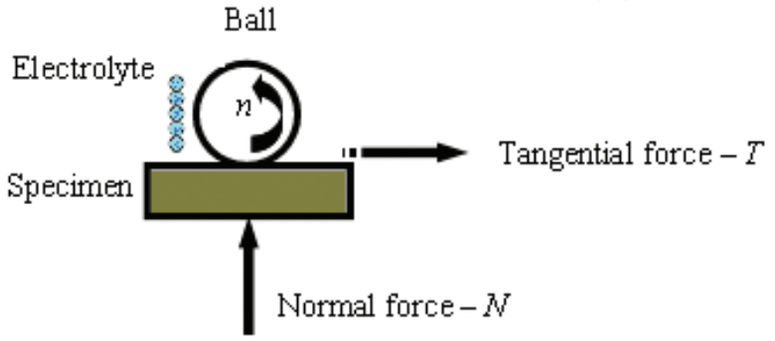

Figure 1. Schematic representation of the operating principle of ball-cratering wear test.

http://dx.doi.org/10.5772/intechopen.73140

electrolyte is supplied between the ball and the specimen during the experiments. The aim of the ball-cratering wear test is to generate "wear craters" on the specimen surfaces. The wear volume (V) may be determined as a function of *b*, using Eq. (1) [12], where *b* is the wear crater diameter and *R* is the ball radius.

$$V \cong \frac{\pi b^4}{64R} \text{ for } b << R \quad (1)$$

Wear tests conducted under the ball-cratering technique present advantages in relation to other types of tests, because it can be performed with normal forces (N) and rotations of the sphere (n) relatively low (N < 0.5 N and n < 80 rpm) [17–21]. Tests in micro- and nanotribometers are used to investigate small regions and thin layers of different surfaces [22, 23].

The aim of this work was to evaluate the cytotoxicity and the tribological behavior of ISO 5832-1 austenitic stainless steel (SS) textured by Yb optical fiber laser, varying its pulse frequency, using two ball-cratering wear methods.

2. Experimental

2.1. Material and sample preparation

The material employed in the present work was a round bar (15 mm diameter) of the ISO 5832-1 austenitic stainless steel (chemical composition in wt%: 0.023 C, 0.78 Si, 2.09 Mn, 0.026 P, 0.0003 S, 18.32 Cr, 2.59 Mo, 14.33 Ni, and Fe balance). Specimens were treated with a nanosecond ytterbium (Yb) optical fiber laser at four different pulse frequencies, as shown in **Table 1**. A pulsed Nd: YAG laser (TRUMARK 5050™) was operated at a wavelength of 1062 ± 3 nm, with a laser average power of 50 W and a scanning speed of 200 mm s^{-1}. **Figure 2** shows the surface finish of the laser-textured specimens.

2.2. Ball-cratering wear test

An instrument with free-ball configuration was used for the sliding wear tests. Two load cells were used in the ball-cratering apparatus: one load cell to control the normal force (N) and one load cell to measure the tangential force (T) developed during the experiments. "Normal" and "tangential" load cells had a maximum capacity of 50 N and an accuracy of 0.001 N. The values of "N" and "T" were registered by a readout system. **Table 2** presents the test conditions selected for the experiments conducted in this work. Balls for the ball-cratering wear test were made of AISI 316L stainless steel, with a diameter of D = 25.4 mm (D = 1″). A phosphate buffer solution (PBS), with chemical composition (g/l): 8.0 NaCl, 0.2 KCl, 1.15 Na_2HPO_4, 0.2 KH_2PO_4, with a pH value of 7.4 and a conductivity of 15.35 mS was dropped between the ball and the specimen.

Specimens	1	2	3	4
Frequencies (kHz)	80	188	296	350

Table 1. Frequencies used for ytterbium optical fiber laser treatment.

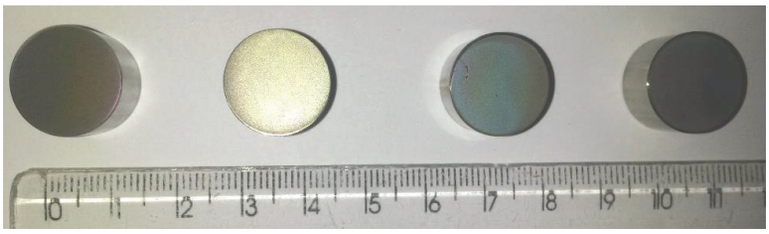

Figure 2. ISO 5832-1 austenitic stainless steel textured by ytterbium optical fiber laser.

Test condition	
(N) Normal force (N)—ball of AISI 316 L SS	0.25
(S) Sliding distance—(m)	8.0
(n) Ball rotational speed—(rpm)	50
(v) Tangential sliding velocity—(m/s)	0.1
(t) Test duration—(min)	10

Table 2. Test conditions selected for the ball-cratering wear experiments.

The values of normal force (N) were defined as a function of the density (ρ) of the ball material (AISI 316 L SS): $\rho_{316L} = 8\ g \cdot cm^{-1}$.

The tests were conducted at t = 10 min. The sliding distance (S) was calculated based on the values of $v = 0.1\ m \cdot s^{-1}$ and t = 10 min (t = 600 s) and was equal to 60 m.

All experiments were conducted without interruption, and the PBS solution was continuously agitated and fed between the ball and the specimen under a frequency of 1 drop/2 s. Both the normal force (N) and the tangential force (T) were monitored and registered constantly. Then, the friction coefficient (μ) was determined using Eq. 2:

$$\mu = \frac{T}{N} \tag{2}$$

2.3. Nanotribometer

The tribological behavior of the ISO 5832-1 austenitic stainless steel was also assessed by wear tests conducted in a nanotribometer (Anton Paar—model NTR²). The tests were performed in the air, at 25°C, with counterbody of chrome steel 52–100 rotating ball shape, 2 mm in diameter, during 10 min, with normal force of 100.0 mN, distance equivalent to 2.4 m, and a scan speed of 4.0 $cm.s^{-1}$. Both laser-textured and pristine materials were evaluated.

2.4. Microhardness (HV)

Vickers microhardness analyses were performed in a microdurometer coupled with optical microscope, Fisherscope HM 2000. The hardness values refer to the average of five measurements at a distance of 50 μm between each indentation, and applied load of 25.0 $mN \cdot 0^{-1}$, for surfaces treated with laser and also for the untreated stainless steel specimens.

http://dx.doi.org/10.5772/intechopen.73140

2.5. Roughness analysis

A LEXT OLS 4100 confocal laser scanning microscope (Olympus, TM) was used in order to obtain the surface roughness of the laser-textured and untreated samples with a higher definition quality in the topographic analysis. The values are expressed as the mean roughness Ra.

2.6. Cytotoxicity analysis

Cytotoxicity was assessed by quantitative methodology. The test is based on the determination of viable cells after exposure of the cell population to the extract obtained from incubation of the samples in cell culture medium RPMI (Gibco®) supplemented with serum bovine fetal 10% and antibiotic/antimycotic (solution Gibco®) 1% at 37°C for 9 days under constant gentle stirring. The long period use was chosen to mimic if the samples were implanted. The treated surface was carefully immersed in cell culture medium to evaluate if there was debris released from the samples that can lead to a cytotoxicity effect. The extract of each sample were used to cultivate on a cell monolayer, CHO (Chinese Hamster Ovarian) cell line for 24 hours.

The analysis of the number of viable cells was performed by the colorimetric method for the metabolization of *supravital* dye, MTS, and the electron coupling agent, PMS (Promega®) were used as the supplier instructions, and subsequently reading in a spectrophotometer at 490 nm. The amount of dye metabolized by the cell population is directly proportional to the number of viable cells on the plate.

3. Results and discussion

3.1. Wear volume analysis

The environment of implants usually induces wear deriving from the contact between the biomaterial and surrounding tissues, so that when manufacturing an implant, one has to choose a suitable area for laser treatment. **Figure 3** shows this biomaterial surface without texturizations (blank).

Figure 4 presents the wear volumes (V) for the untreated and laser-textured samples after the ball-cratering wear tests. These values were determined according to Eq. (1). It is possible to observe that the wear volume decreased for the laser-textured specimens with respect to the untreated steel. This fact is likely to be associated with an increase in the surface hardness after laser texturing. As shown in **Table 3**, the microhardness of the laser-textured samples was higher than that of the untreated material. The highest values of wear volume were obtained for the untreated specimens. The wear resistance of the laser-textured surfaces was superior to that of the pristine material. Similar results were reported by Cozza et al. [13] using the same test for a different tribological system.

Microstructural and topographic modifications due to changes in some parameters of the laser beam were identified by Lima et al. [24]. They used a Q-switched Nd: YAG laser with different pulse frequencies. Similarly, they performed texturing treatment that consisted of

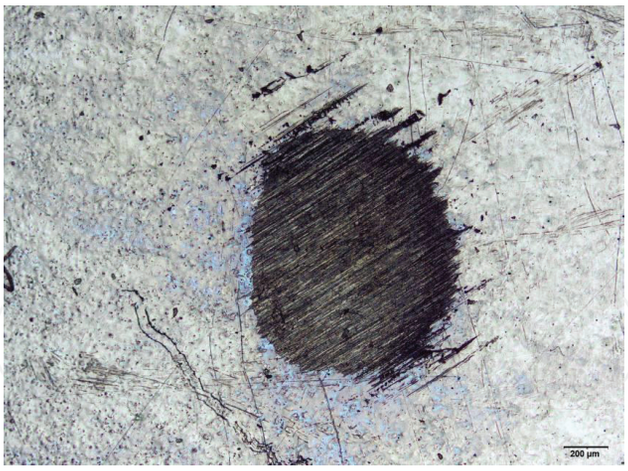

Figure 3. Wear test conducted on the ISO 5832-1 SS without laser treatment. Ball of AISI 316 L SS.

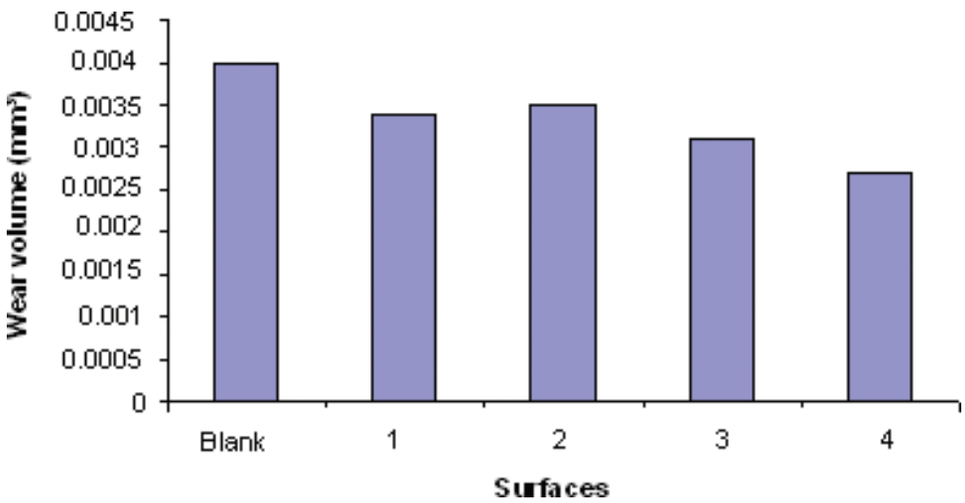

Figure 4. Wear volumes of the untreated and laser-textured surface determined after the ball-cratering wear tests.

juxtaposed lines on the surface of the AISI M2 tool steel. Changes in beam energies and intensities were observed. All conditions used produced metal fusion. They noticed that there was little roughness for the low intensities generated by the laser beam; however, there were "craters", that is, regions with high roughness at the higher intensities.

Allsopp and Hutchings [25] have suggested that surface roughness is interesting for improving adhesion between coatings and metallic alloys, and can be produced and controlled by laser beam. This effect is desirable on some biomaterials' surfaces for permanent fixture medical devices. The values of Ra shown in **Table 3** reveal that the average roughness increased after laser texturing, scaling up with the pulse frequency.

Specimens	**Blank**	**1**	**2**	**3**	**4**
Microhardness (HV)	199.3	204.3	215.4	226.1	239.9
Ra (µm)	0.2	1.5	5.2	9.2	11.5

Table 3. Microhardness and roughness values for the untreated and laser-textured samples.

3.2. Friction coefficient

Because wear is a surface phenomenon that occurs at the interface between the asperities of the surfaces in contact, biotribology results are strongly influenced by the surface finish produced by the laser beam texturing.

Considering the ball-cratering wear test, the highest value of the friction coefficient was obtained for the untreated surface as shown in **Figure 5**. The laser-textured specimens presented lower friction coefficient. The lowest value was observed for specimen 3. There was no apparent relationship between the friction coefficient and the laser pulse frequency. Notwithstanding, it is possible to infer that the hardness increase can be related to this effect. Surface roughness, in turn, did not increase the friction coefficient, being the hardness effect more prominent to the friction characteristics of the treated surface. Values of such magnitudes were reported in literature [25–28], with the same type of test under different tribological systems.

In the biomaterials' field for implantable medical or dental devices, tribological assays are of great value in providing an estimate of the normal, tangential, and frictional forces in relation to the volume of material that can be detached from the surface, migration, and accommodation of some particles.

This work also analyzed the evolution of the friction coefficient by nanotribometer wear tests of the surfaces of these biomaterials with laser texturing treatment. The results obtained are presented in **Figure 6**, and are compared with the blank specimen (without treatment).

No direct relationship between wear volume and friction coefficient was observed; i.e., the highest value of wear volume was not related to the higher value of coefficient of friction [25–28].

The variation of the friction coefficient with the test time is shown in **Figure 6** for the laser-textured and untreated samples. These results were obtained by means of the wear tests conducted in the nanotribometer. For the laser-textured surfaces, the values of friction coefficient were lower than those obtained for untreated surface, confirming the results of the ball-cratering wear test.

For the laser-textured surfaces, **Figure 6**, the values of friction coefficient obtained were lower than those obtained in the samples without treatment by the laser beam (blank).

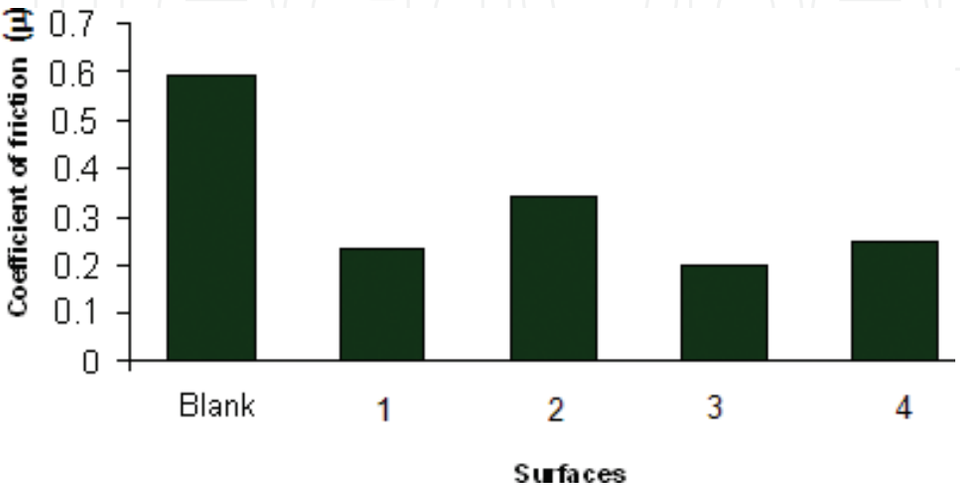

Figure 5. Friction coefficient obtained by the ball-cratering wear test for untreated and textured specimens.

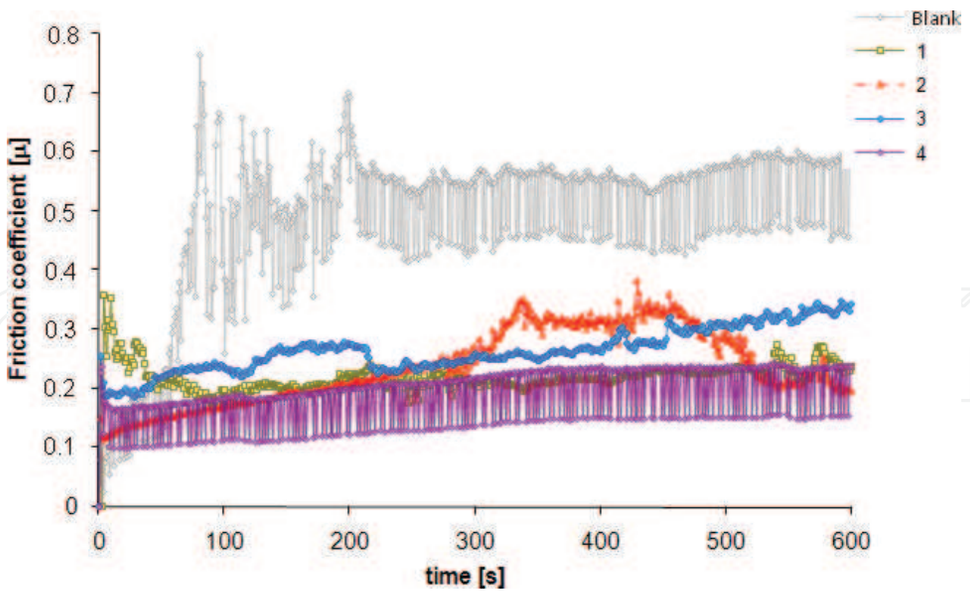

Figure 6. Variation of friction coefficient as a function of the test time for the laser-textured and -untreated specimens.

The friction coefficient values for the untreated specimen showed a rapid increase in the beginning of the test (running-in), and practically stabilized around values close to μ = 0.5 as the surface becomes less rough. In the case of the laser-textured samples, the friction coefficient decreases up to 100 s, reaching a stabilization period up to the end of the test. For sample 2, the friction coefficient initially presented gradual increase up to 500 s reaching 0.35 and then drops to less than 0.2 at the end of the test. Sample 3 showed a tendency of continuous increment of the friction coefficient with time. For sample 4, in turn, it remained practically constant and at lower than that of the other conditions.

The effect of the variation of the coefficient of friction as a function of the test time was studied by Huang et al. [29]. They verified some tribological properties of Ti-6Al-4 V alloys with and without coating ("laser clad"), for a period of 3500 s in different rotation frequencies, and at the end of the tests, they verified that the coefficient of friction for the coatings was always inferior to the substrate.

3.3. Cytotoxicity analysis

The results presented in **Figure 7** indicate that the austenitic ISO 5832-1 SS exhibited cytotoxic behavior similar to the negative control, that is, it shows no cytotoxicity. This is indicated by the cell viability curve for the laser-treated samples above the level $IC_{50\%}$ of cytotoxicity. **Table 4** shows the pH of the extracts at a concentration of 100%.

The cytotoxicity of the ISO 5832-1 stainless steel was evaluated in the present study according to ISO 10993-5 [30]. The absence of cytotoxicity is desired for stainless steels for medical and dental applications [31]. The slight decrease in the cell viability for the laser-treated samples

http://dx.doi.org/10.5772/intechopen.73140

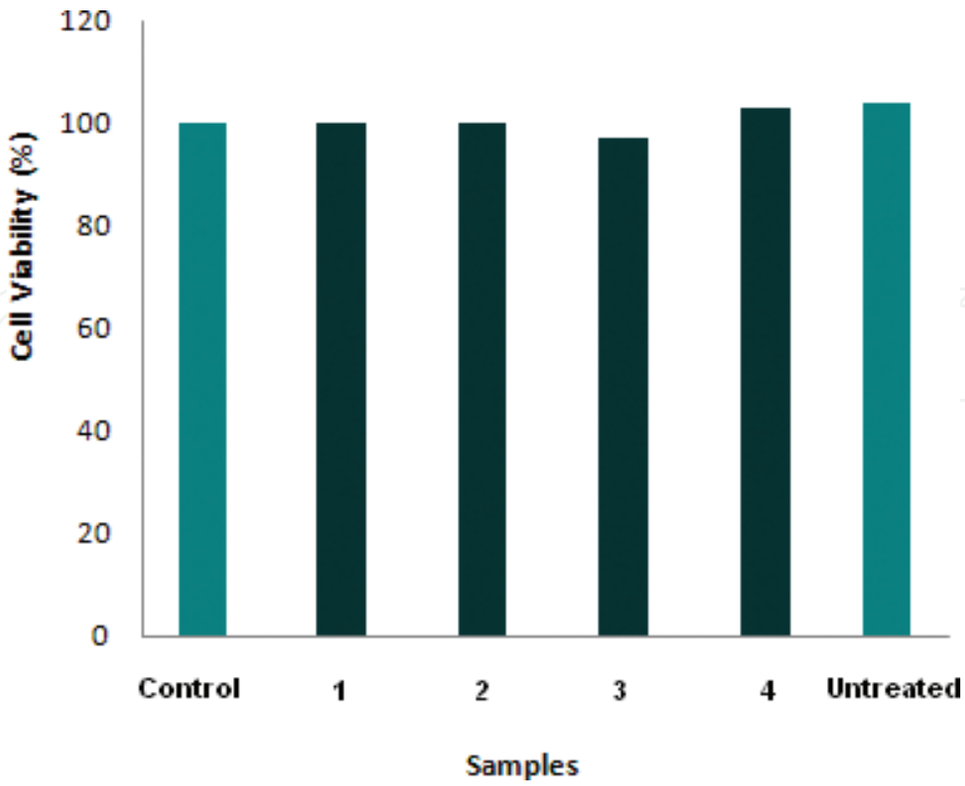

Figure 7. Cell viability as a function of the extract concentration of the laser-textured and untreated samples.

Extracts	pH
Control (Pure Ti)	7.50
ISO 5832-1 SS treated by laser	7.88

Table 4. Values of pH for the extracts at a concentration of 100%.

is explained by its susceptibility to localized corrosion [5, 6, 32, 33]. According to Pieretti and Costa [5], the laser process affects the corrosion resistance of the laser-treated stainless steel biomaterials, producing a less protective passive film with areas prone to its breakdown, although the samples are not considered cytotoxic.

Studies on the biomaterials tribological behavior are important because they reveal unique aspects about the surface wear mechanisms [34]. The knowledge of wear response contributes to the understanding of other surface phenomena, which can occur simultaneously and potentiate one another, such as the phenomenon of corrosion.

The occurrence of both concomitantly can lead to acceleration of particle detachment, including nonmetallic inclusions that may be housed under biomaterial surface [35], and these may come into contact with the bloodstream and lodge in any part of the human body causing, many times, harm to the patients.

4. Conclusions

In this work, surface texturing of ISO 5832-1 stainless steel samples was carried out using an optical fiber Yb laser. The effect of the laser pulse frequency on the tribological behavior of the treated steel was evaluated by ball-cratering wear tests and sliding wear tests using a nano-tribometer. The wear volume determined from the ball-cratering wear test points out that the laser-textured surfaces were more resistant to wear, presenting lower wear volumes than the untreated material. The friction coefficient decreased after laser texturing likely due to the increased surface hardness of the laser-treated samples as revealed by Vickers microhardness measurements. This effect was observed for the wear tests conducted with the ball-cratering apparatus and the nanotribometer. The laser texturing process did not impart any cytotoxicity to the ISO 5832-1 samples, preserving the biocompatibility of the pristine surface.

Acknowledgements

The authors acknowledge CNPq for the financial support, under grant number Process: 350798/2014-1, Project: 459565/2013-3, and Dr. R. C. Cozza.

Author details

Eurico Felix Pieretti[1]*, Andrea Cecília Dorión Rodas[2], Renato Altobelli Antunes[2] and Maurício David Martins das Neves[1]

*Address all correspondence to: efpieretti@usp.br

1 Nuclear and Energy Research Institute (IPEN-CNEN), São Paulo, SP, Brazil

2 Federal University of ABC (UFABC), Santo André, SP, Brazil

References

[1] Okasaki Y. Effect of friction on anodic polarization properties of metallic biomaterials. Biomaterials. 2002;**23**:2071-2077

[2] Black J. Systemic effects of biomaterials. Biomaterials. 1984;**5**:11-18

[3] Anderson JM. Biological response to materials. Annual Review of Materials Research. 2001;**31**:81-110

[4] ISO 5832-1:2016, Implants for Surgery - Metallic Materials - Part 1: Wrought Stainless Steel

[5] Pieretti EF, Costa I. Surface characterisation of ASTM F139 stainless steel marked by laser and mechanical techniques. Electrochimica Acta. 2013;**114**:838-843

[6] Pieretti EF, Manhabosco SM, Dick LFP, Hinder S, Costa I. Localized corrosion evaluation of the ASTM F139 stainless steel marked by laser using scanning vibrating electrode technique, X-ray photoelectron spectroscopy and Mott-Schottky techniques. Electrochimica Acta. 2014;**124**:150-155

[7] Pieretti EF, Palatnic RP, Leivas TP, Costa I, Neves MDM. Evaluation of laser marked ASTM F 139 stainless steel in phosphate buffer solution with albumin. International Journal of Electrochemical Science. 2014;**9**:2435-2444

[8] Pieretti EF, Costa I, Marques RA, Leivas TP, Neves MDM. Electrochemical study of a laser marked biomaterial in albumin solution. International Journal of Electrochemical Science. 2014;**9**:3828-3836

[9] Adachi K, Hutchings IM. Wear-mode mapping for the micro-scale abrasion test. Wear. 2003;**255**:23-29

[10] Stachowiak GB, Stachowiak GW, Celliers O. Ball-cratering abrasion tests of high-Cr white cast irons. Tribology International. 2005;**38**:1076-1087

[11] Stachowiak GB, Stachowiak GW, Brandt JM. Ball-cratering abrasion tests with large abrasive particles. Tribology International. 2006;**39**:1-11

[12] Rutherford KL, Hutchings IM. Theory and application of a micro-scale abrasive wear test. Journal of Testing and Evaluation - JTEVA. 1997;**25**(2):250-260

[13] Cozza RC, Tanaka DK, Souza RM. Friction coefficient and abrasive wear modes in ball-cratering tests conducted at constant normal force and constant pressure – Preliminary results. Wear. 2009;**267**:61-70

[14] Cozza RC, de Mello JDB, Tanaka DK, Souza RM. Relationship between test severity and wear mode transition in micro-abrasive wear tests. Wear. 2007;**263**:111-116

[15] Cozza RC. Influence of the normal force, abrasive slurry concentration and abrasive wear modes on the coefficient of friction in ball-cratering wear tests. Tribology International. 2014;**70**:52-62

[16] Trezona RI, Allsopp DN, Hutchings IM. Transitions between two-body and three-body abrasive wear: Influence of test conditions in the microscale abrasive wear test. Wear. 1999; **225**-**229**:205-214

[17] Cozza RC, Tanaka DK, Souza RM. Friction coefficient and wear mode transition in micro-scale abrasion tests. Tribology International. 2011;**44**:1878-1889

[18] Cozza RC. A study on friction coefficient and wear coefficient of coated systems submitted to micro-scale abrasion tests. Surface & Coatings Technology. 2013;**215**:224-233

[19] Bose K, Wood RJK. Optimum tests conditions for attaining uniform rolling abrasion in ball cratering tests on hard coatings. Wear. 2005;**258**:322-332

[20] Axén N, Jacobson S, Hogmark S. Influence of hardness of the counterbody in three-body abrasive wear – An overlooked hardness effect. Tribology International. 1994;**27**(4):233-241

[21] Gee MG, Wicks MJ. Ball crater testing for the measurement of the unlubricated sliding wear of wear-resistant coatings. Surface and Coatings Technology. 2000;**133-134**:376-382

[22] Sun D, Wharton JA, Wood RJK. Micro-abrasion mechanisms of cast CoCrMo in simulated body fluids. Wear. 2009;**267**:1845-1855

[23] Wood RJK, Sun D, Thakare MR, de Frutos Rozas A, Wharton JA. Interpretation of electrochemical measurements made during micro-scale abrasion-corrosion. Tribology International. 2010;**43**:1218-1227

[24] Lima MSF, Vieira ND Jr, Morato SP, Vencovsky P. Microstructural changes due to laser ablation of oxidized surfaces on an AISI M2 tool steel. Materials Science and Engineering A. 2003;**344**:1-9

[25] Allsopp DN, Hutchings IM. Micro-scale abrasion and scratch response of PVD coatings at elevated temperatures. Wear. 2001;**251**:1308-1314

[26] Adachi K, Hutchings IM. Sensitivity of wear rates in the micro-scale abrasion test to test conditions and material hardness. Wear. 2005;**258**:318-321

[27] Cozza RC. Effect of the pressure on the abrasive wear modes transitions in micro-abrasive wear tests of WC-co P20. Tribology International. 2013;**57**:266-271

[28] Adachi K, Hutchings IM. Wear-mode mapping for the micro-scale abrasion test. Wear. 2003;**255**:23-29

[29] Huang C, Zhang Y, Vilar R, Shen J. Dry sliding wear behavior of laser clad TiVCrAlSi high entropy alloy coatings on Ti-6Al-4V substrate. Materials and Design. 2012;**41**:338-343

[30] ISO 10.993 - Biological Evaluation of Medical Devices - Part 5: Tests for Cytotoxicity: *In vitro* Methods; 1992. pp. 1-7

[31] Marques RA, Rogero SO, Terada M, Pieretti EF, Costa I. Localized corrosion resistance and cytotoxicity evaluation of Ferritic stainless steels for use in implantable dental devices with magnetic connections. International Journal of Electrochemical Science. 2014;**9**:1340-1354

[32] Pieretti EF, Pessine EJ, Correa OV, Rossi W, Neves MDM. Effect of laser parameters on the corrosion resistance of the ASTM F139 stainless steel. International Journal of Electrochemical Science. 2015;**10**:1221-1232

[33] Pieretti EF, Neves MDM. Laser marked and textured biomaterial evaluated by Mott-Schottky technique. International Journal of Electrochemical Science. 2017;**12**:9204-9211

[34] Duisabeau L, Combrade P, Forest B. Environmental effect on fretting of metallic materials for orthopaedic implants. Wear. 2004;**256**:805-816

[35] Pieretti EF, Neves MDM. Influence of laser marks on the electrochemical behaviour of the ASTM F139 stainless steel for biomedical application. International Journal of Electrochemical Science. 2016;**11**:3532-3541